UNDERCUTTING ON CAM PROFILES

Chao Chen
cchen@mie.utoronto.ca
Department of Mechanical & Industrial Engineering University of Toronto, Ontario

Jorge Angeles
angeles@cim.mcgill.ca
Department of Mechanical Engineering McGill University, Montreal

Received March 2006, Accepted October 2006
No. 06-CSME-15, E.I.C. Accession 2934

ABSTRACT

This paper discusses the technology of undercutting on cam profiles to improve the transmission quality in cam-based speed-reducers. By means of the contact ratio and the pressure angle, two principles for undercutting are established to ensure a feasible mechanism. Polynomials are applied to generate the undercutting curves to satisfy our requirements. Finally, an example is given to illustrate the methodology.

COUPE DE CAMES PAR ÉVIDEMENT

RESUME

Cet article présente la coupe par évidement de profils de cames et explique en quoi cette technique permet d'améliorer la qualité des réducteurs à cames. Deux principes de coupe par évidement, définis à partir du ratio de contact et de l'angle de pression, assurent la faisabilité du mécanisme. Les auteurs utilisent des polynômes pour déterminer les courbes de coupe qui satisfont leurs exigences. Un exemple illustre cette méthode.

1 INTRODUCTION

Cams are widely used in many dynamical systems to move loads with smooth starts and stops. Different methods have been applied to design cam profiles [1, 2, 3].

The cam mechanism studied here is called Speed-o-Cam (SoC), which was designed based on the synthesis paradigm proposed in [4, 5]. Such mechanisms are composed of a cam, a follower supplied with rollers, and a fixed frame. The spatial cam profile is determined under non-slip conditions by means of the three-dimensional Aronhold-Kennedy Theorem, thereby reducing the power losses caused by friction. The novel mechanical transmissions offer low backlash, high efficiency, high reduction ratio, and high stiffness, as compared to conventional transmissions such as gears, harmonic drives, etc. [6].

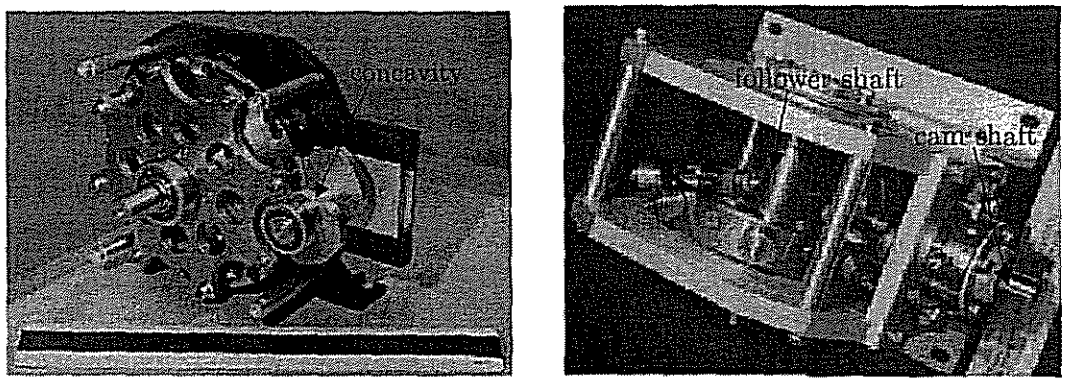

(a) (b)

Figure 1: (a) Planar SoC with one concavity; (b) spherical SoC

Prototypes of SoC are displayed in Fig. 1, where: (a) features a cam plate exhibiting a concavity, with a reduction ratio of 8:1; (b) a spherical mechanism with a reduction ratio of 8:1, whose input and output axes intersect at 90° and whose cams have convex contact surfaces. The geometry of planar cams is recalled in Subsection 2.1, that of their spherical counterparts in Subsection 2.2.

Undercutting on SoC was discussed by Zhang [7], who applied 2-4-6 and 2-4-6-8 polynomials to generate the *undercutting curve*. This approach entails some disadvantages, namely,

- Criteria to select the blending points between cam profiles and undercutting curve are lacking;
- The degree of the interpolating polynomial is unnecessarily high;
- The undercutting curve is not guaranteed to lie inside the original cam profile.

The procedure discussed here is intended to eliminate these drawbacks.

2 CAM PROFILE

A systematic generation and analysis of contact surfaces of the SoC cams can be found in [4], where spatial-cam contact surfaces are produced from dual vectors. The planar and spherical profiles

are produced from the dual and the primal parts of the dual vectors, respectively. The spatial cam mechanism is not practical yet, because of the translation of the roller, bearing the shape of a hyperboloid, on the follower along its pin. Therefore, we limit the discussion to planar and spherical cams here.

2.1 Planar Cams

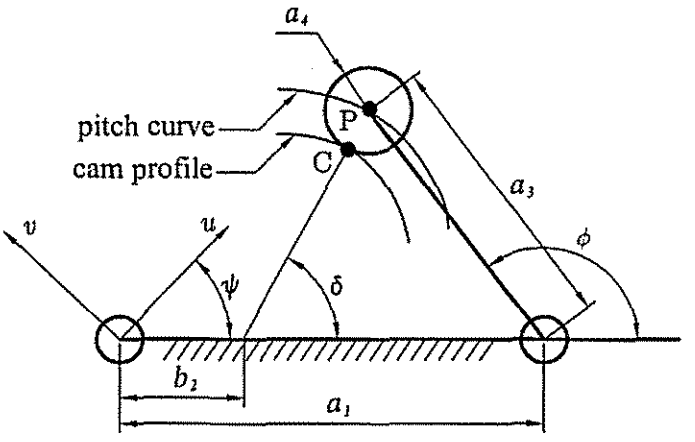

Figure 2: The pertinent notation of a planar cam

The notation of a planar cam, introduced in Fig. 2, is needed to define the planar cam profile:

ψ: angle of rotation of the cam

ϕ: angle of rotation of the follower

ϕ': derivative of ϕ with respect to ψ

a_1: distance between input and output axes

a_3: distance between output and roller axes

a_4: radius of the roller

N: number of the rollers on the follower

The input-output function for a constant speed reduction of $N:1$ is given by [8]

$$\phi = -\pi\left(1 - \frac{1}{N}\right) - \frac{\psi}{N} \tag{1}$$

The *pitch curve* is given by the trajectory of the centre P of the roller in the moving frame attached on the cam, of coordinates (u_p, v_p), namely,

$$u_p = a_1\cos(\psi) + a_3\cos(\phi - \psi) \tag{2a}$$

$$v_p = -a_1\sin(\psi) + a_3\sin(\phi - \psi) \tag{2b}$$

The coordinates of the contact point C, on the cam profile, in the moving frame are given in turn by:

$$u_c = u_p + a_4 \cos(\delta - \psi + \pi) \tag{3a}$$

$$v_c = v_p + a_4 \sin(\delta - \psi + \pi) \tag{3b}$$

$$b_2 = \frac{1}{1+N} a_1 \tag{3c}$$

$$\delta = \arctan\left(\frac{a_3 \sin\phi}{a_3 \cos\phi + a_1 - b_2}\right) \tag{3d}$$

where eq. (3c) is derived from the Aronhold-Kennedy Theorem [9, 10].

2.2 Spherical Cams

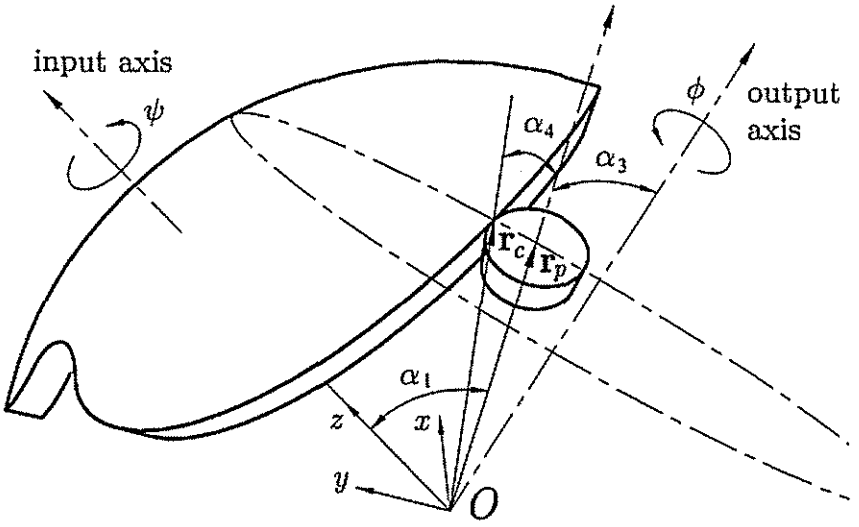

Figure 3: The pertinent notation of a spherical cam

A spherical cam is shown in Fig. 3, the notation needed to define the *conical* contact surface being given below:

ψ: angle of rotation of the cam

ϕ: angle of rotation of the follower

ϕ': derivative of ϕ with respect to ψ

α_1: angle between input and output axes

α_3: angle between output and roller axes

α_4: angle of the roller cone

N: number of the rollers on the follower

The input-output function for a constant speed reduction of $N:1$ is given by

$$\phi = \pi\left(1 - \frac{1}{N}\right) + \frac{\psi}{N} \tag{4}$$

The pitch curve in the moving frame attached on the cam is a conic surface generated by a unit vector $\mathbf{r}_p$ along the axis of the roller as this moves around the axis of the cam, which is given by

$$\mathbf{r}_p = \lambda \begin{bmatrix} \sin\alpha_3 \sin\phi \cos\psi - k_1 \sin\psi \\ -\sin\alpha_3 \sin\phi \sin\psi - k_1 \cos\psi \\ \cos\alpha_1 \cos\alpha_3 - \sin\alpha_1 \sin\alpha_3 \cos\phi \end{bmatrix} \tag{5}$$

where λ is a scalar yielding a unit vector, and

$$k_1 = \sin\alpha_1 \cos\alpha_3 + \cos\alpha_1 \sin\alpha_3 \cos\phi \tag{6}$$

is the negative of the y-component of $\mathbf{r}_p$ in the machine frame.

The contact surface in the moving frame is given in turn by a unit vector $\mathbf{r}_c$ pointing from the sphere centre to the contact point, namely,

$$\mathbf{r}_c = \lambda \begin{bmatrix} \sin(\theta_3 - \alpha_4)\sin\delta\cos\psi - k_2 \sin\psi \\ -\sin(\theta_3 - \alpha_4)\sin\delta\sin\psi - k_2 \cos\psi \\ \cos\theta_2 \cos(\theta_3 - \alpha_4) - \sin\theta_2 \sin(\theta_3 - \alpha_4)\cos\delta \end{bmatrix} \tag{7}$$

where

$$k_2 = \sin\theta_2 \cos(\theta_3 - \alpha_4) + \cos\theta_2 \sin(\theta_3 - \alpha_4)\cos\delta \tag{8a}$$

$$\tan\theta_2 = \frac{\phi' \sin\alpha_1}{\phi' \cos\alpha_1 - 1} \tag{8b}$$

$$\tan\theta_3 = \frac{\sqrt{[\cos(\alpha_1 - \theta_2)\phi \sin\alpha_3 + \cos\alpha_3 \sin(\alpha_1 - \theta_2)]^2 + \sin^2\alpha_3 \sin^2\phi}}{\cos\alpha_3 \cos(\alpha_1 - \theta_2) - \cos\phi \sin\alpha_3 \sin(\alpha_1 - \theta_2)} \tag{8c}$$

$$\tan\delta = \frac{\sin\alpha_3 \sin\phi}{\sin\alpha_3 \cos(\alpha_1 - \theta_2)\cos\phi + \cos\alpha_3 \sin(\alpha_1 - \theta_2)} \tag{8d}$$

in which k_2 is the negative of the y-component of $\mathbf{r}_c$ in the machine frame. Moreover, if points P_3, P_{32} and P_{43} are defined on the unit sphere centred at the centre of the mechanism, then a spherical triangle is obtained whereby $\delta = \angle P_3 P_{32} P_{43}$ and $\theta_3 = \widehat{P_3 P_{43}}$ measured from P_3 to P_{43}. Here, P_3 and P_{43} lie on the axes of the roller and the follower, respectively, while P_{32} on the contact element of the follower-cam pair.

3 PRESSURE ANGLE

The pressure angle is an important index to evaluate the force-transmission quality. In cam mechanisms, the pressure angle depends on the driving mode, which can be either direct or inverse. The *direct operation* is defined as that in which the cam is the driving element, the *inverse operation* being that in which the cam is the driven element [4].

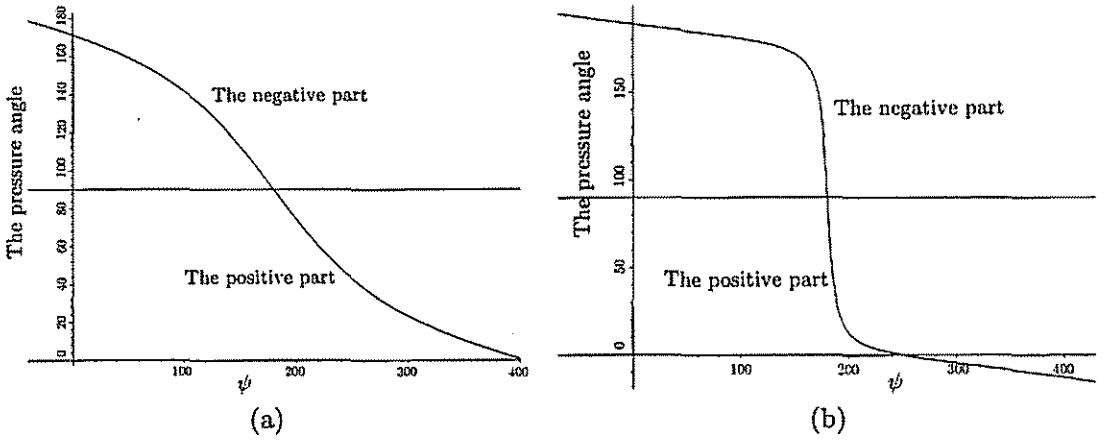

Figure 4: The pressure angle of (a) a planar SoC with a speed-reduction of 6:1 and (b) a spherical SoC with a speed-reduction of 3:1

By means of dual-number algebra and the Aronhold-Kennedy Theorem, the pressure angle of the spatial cam transmission is given by [4]

$$\tan\mu = \frac{\sqrt{A\lambda^4 + B\lambda^3 + C\lambda^2 + D\lambda + E}}{F\lambda^2 + G\lambda + H} \tag{9}$$

where $A, B, ..., H$ are the functions of the design parameters, with λ measured along the generatrix of the pitch ruled surface. The details are included in the Appendix.

The pressure angle in a planar SoC is given by

$$\tan\mu = \frac{a_3(\phi' - 1) - a_1\cos\phi}{a_1\sin\phi} \tag{10}$$

As shown in Fig. 4(a), we notice that part of the curve lies above 90°, around which value the cam cannot drive the follower. We shall call this part of the cam profile the *negative part*. Similarly, the *positive part* is that part of the cam profile which yields a pressure angle smaller than 90°.

In the case of spherical SoC, the pressure angle is given by

$$\tan\mu = \frac{(\phi' - \cos\alpha_1)\sin\alpha_3 - \sin\alpha_1\cos\alpha_3\cos\phi}{\sin\alpha_1\sin\phi} \tag{11}$$

The plot of the pressure angle is shown in Fig. 4(b). Similarly, the spherical cam profile also comprises two parts: the negative part and the positive part.

4 CONTACT RATIO

It is apparent from the plots of Figs. 4 that the pressure angle attains values from 0 to π. This means that one single cam cannot possibly drive its follower throughout one complete cycle, which brings about the need of at least one second, conjugate cam. Before one cam profile ceases action, its conjugate counterpart must already have come into engagement. This overlapping is essential.

A measure of such overlapping in gear transmissions is the *contact ratio*, which is defined, for gears, as the ratio of the angle of action to the pitch angle [11]. Therefore, the contact ratio in one gear pair is given by $\kappa = \theta/\gamma$ where γ is the pitch angle, and θ is the angle of action [11].

It is good design practice to maintain a contact ratio of 1.2 or greater. A gear contact ratio between 1 and 2 means that part of the time two pairs of teeth are in contact; during the remaining time one single pair is in contact. We can apply the foregoing definition directly to the case of SoC.

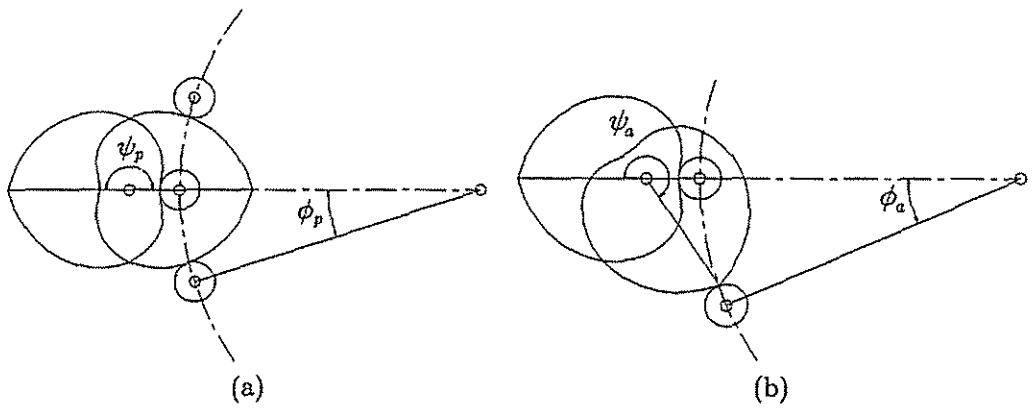

Figure 5: The contact ratio in a planar SoC

Figure 5 shows the geometry of a planar SoC. The angle of action can be defined with respect to the input angle ψ and the output angle ϕ, respectively. The same applies to the pitch angle. Hence, we have

$$\kappa_1 = \frac{\psi_a}{\psi_p}, \quad \kappa_2 = \frac{\phi_a}{\phi_p} \tag{12}$$

where ψ_a and ψ_p are the angle of action and the pitch angle of the input, ϕ_a and ϕ_p being those of the output. Since SoCs are constant-ratio speed reducers, we must have $\kappa_1 = \kappa_2$.

Furthermore, the contact ratio can best be illustrated by means of the plot of the pressure angle occurring in a planar SoC, as shown in Fig 6(a), where the contact ratio turns out to be

$$\kappa = 1.23 \tag{13}$$

The contact ratio in a spherical SoC mechanism can be derived directly from the definition for a planar SoC. Figure 6(b) shows the angle of action and the pitch angle of a spherical SoC. Hence, the contact ratio is given by

$$\kappa = 1.39 \tag{14}$$

We have thus shown, with the aid of the plots of Fig. 6, that SoC designs are possible with contact-ratio values above the minimum adopted for gear trains.

5 UNDERCUTTING OF THE CAM PROFILE

During the contact-overlapping between cam and follower, the mechanisms becomes statically indeterminate. Shown in Fig. 7 are the pressure-angle distributions of the two conjugate cams,

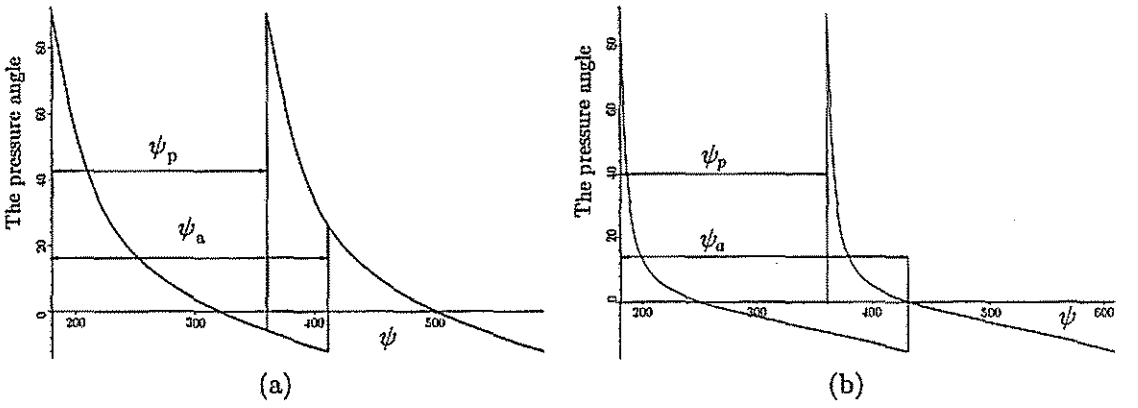

Figure 6: The contact ratio of (a) a planar SoC with a speed-reduction of 8 : 1 and (b) a spherical SoC with a speed-reduction of 3 : 1

where the dashed areas indicate the contact-overlapping. The plot of Fig. 7 is essential to assess the amount of contact-overlapping, which impacts the transmission quality of the mechanism. Usually, engineers consider the smaller pressure angle as the overall transmission performance [5], since they believe that the cam with the smallest pressure angle will contribute the most power to the follower. However, this should be taken with a grain of salt because it is possible that only one cam, even one with a high pressure angle, come into engagement, due to machining and assembly errors. In this case, the likelihood of poor force-transmission quality, and even jamming, increases. In order to reduce this likelihood, we need to *undercut* the cam profile. Undercutting is a trade-off task, which aims at improving the transmission performance, while keeping a large-enough contact ratio.

5.1 Blending Points

We can define four blending points, C, D, F and G, and two offset points, E and H, on the cam profile, as shown in Fig. 8(a). We use primes to indicate the corresponding points on the conjugate cam, cam 2, as shown in Fig. 8(b).

5.1.1 Concavity Point

The concavity point B of a cam is shown in Fig. 8(a). The purpose of undercutting around the concavity point is to avoid a too high pressure angle. To this end, we introduce:
Principle 2.1: *Admissible values of the pressure angle are those below* 60°.

Notice that 60° is not the maximum value of the pressure angle, which can be much lower than this value during transmission. The value of 60° is set as an upper bound of the pressure angle, to prevent transmission singularities, i.e., a pressure angle of 90°.

According to Principle 2.1, we cut the part of cam with the pressure angle over 60°, as shown in Fig. 8(b). The point F′ is the blending point associated with the concavity point B′, and hence, F′ is the new start point of the engagement. G′ will be the symmetric point of F′ with respect to the u axis, H′ being the offset point of B′ along the u axis, as depicted in Fig. 8(a). The offset distance d will be determined presently.

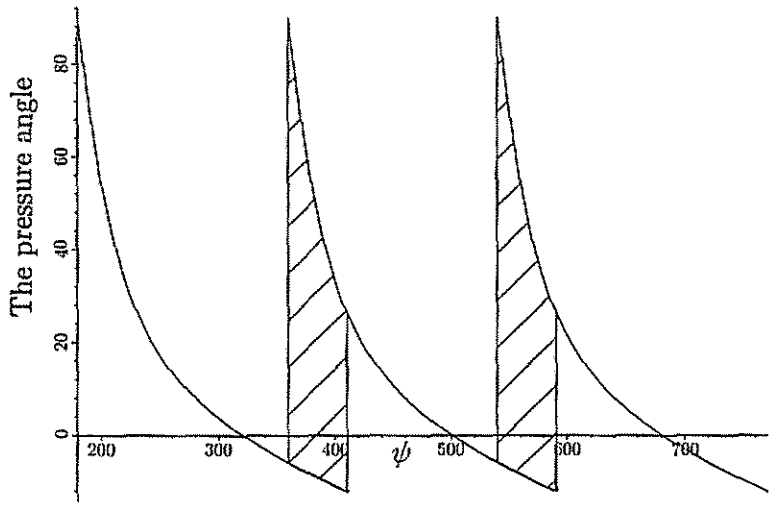

Figure 7: The overlapping of the force transmission

5.1.2 Cusp Point

The cusp[1] point A of a cam is shown in Fig. 8(a). The cusp point has an infinite curvature, and hence, clanking noise and vibration occur due to impact and compressive stress at this point. We need to round the cusp point to solve this problem. On the other hand, we do not want to cut too much because the pressure angle around the cusp point is quite small. Therefore, we choose $10\% \sim 20\%$ of $\psi_4 - \psi_2$ from point A to determine the blending point D, as shown in Fig. 8(a). C is the symmetric point of D with respect to the u axis, E being the offset point of D along the same axis, as depicted in Fig. 8(a). The offset d is given by

$$d = (u_A - u_D)k \tag{15}$$

where k is chosen between 10% and 20% according to experience, in order to prevent contact and a concave cusp point. Applying the same d, we also obtain E′ around the concavity point.

It has been widely accepted that under no circumstances should the contact ratio drop below 1.1, calculated for all tolerances at their worst-case values [11]. Hence, we have

Principle 2.2: *The admissible contact ratio in a SoC transmission after undercutting is greater than* 1.1.

If a pair of conjugate cams cannot satisfy the two foregoing principles, we declare that the cam profile is unfeasible.

5.2 Undercutting Curve

Second-order geometric continuity, termed G^2-*continuity*, at the blending points is desired to smooth the blending of cam profile and undercutting curve in spite of machining and assembly errors.

[1]Strictly speaking, a *cusp* in a curve is defined as a point at which the curvature is discontinuous, although the tangent is continuous. We use here "cusp" rather loosely.

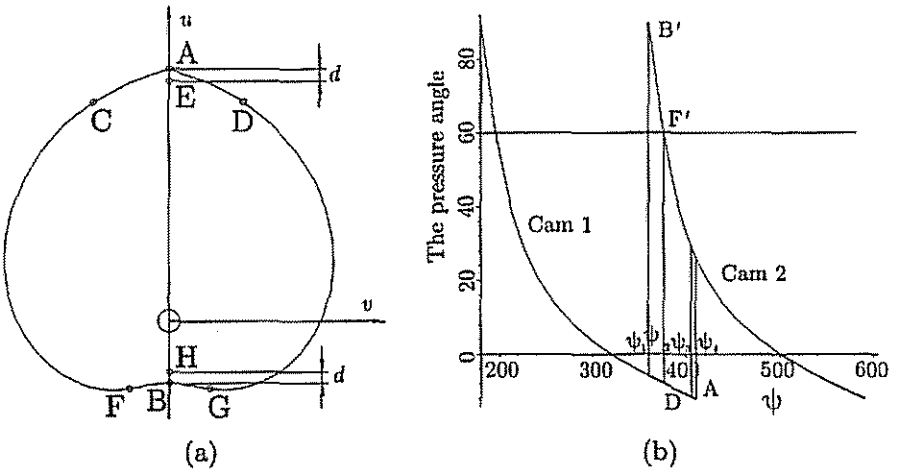

Figure 8: The blending and offset points on (a) a planar cam profile and (b) the plot of the pressure angle

Polynomials are chosen to generate the undercutting curve. We try to use the lowest-degree polynomial to satisfy the blending conditions in order to reduce the complexity of the curve.

5.2.1 Concavity Point

Given the symmetric structure of the cam, we only need to generate half of the curve, from H to G, and then, mirror it with respect to the u axis. We want to avoid a sharp angle at the concave point H, which would be difficult to machine. Therefore, the derivative of the interpolating polynomial with respect to v should vanish at H.

We have a total of five blending conditions, which need five parameters to satisfy. Hence, we use a fourth-order polynomial, as given by

$$u = g_4 v^4 + g_3 v^3 + g_2 v^2 + g_1 v + g_0 \quad (16a)$$

$$u' = 4g_4 v^3 + 3g_3 v^2 + 2g_2 v + g_1 \quad (16b)$$

$$u'' = 12g_4 v^2 + 6g_3 v + 2g_2 \quad (16c)$$

5.2.2 Cusp Point

In this case, we only want position-continuity at E, because a sharp angle at the convex point E is not a problem for machining. Moreover, since point E will never contact the follower, the Hertz stresses are not an issue. Furthermore, the second-order continuity at E has the potential to force the curve to go outside of the original cam profile, as shown in Fig. 9, which will perturb the uniform transmission ratio.

Therefore, only four initial conditions are required in this problem, which can be satisfied by a cubic polynomial.

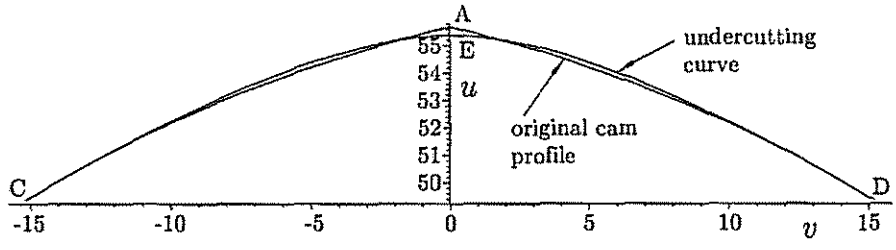

Figure 9: The undercutting curve with a segment lying outside of the original cam profile

$$u = g_3 v^3 + g_2 v^2 + g_1 v + g_0 \tag{17a}$$
$$u' = 3g_3 v^2 + 2g_2 v + g_1 \tag{17b}$$
$$u'' = 6g_3 v + 2g_2 \tag{17c}$$

6 EXAMPLE

One planar SoC is studied here, as an example:

$$a_1 = 130 \text{ mm} \quad a_3 = 105 \text{ mm} \quad a_4 = 8 \text{ mm} \quad N = 8 \tag{18}$$

where the parameters are shown in Fig. 2. The cam profile before undercutting with the blending points and the pressure angle of the conjugate cams are depicted in Figs. 8(a) and (b), respectively. The contact ratio after undercutting is given by

$$\kappa = \frac{\psi_a}{\psi_p} = 1.12 \tag{19}$$

Therefore, this cam profile obeys Principle 2.2. Assuming $k = 20\%$, the offset d, as given by eq. (15), is

$$d = 0.295\text{mm} \tag{20}$$

thereby determining the offset points E and H. Now we can generate the undercutting curves around the cusp point and the concavity point. At the cusp point, the cubic polynomial given by eq. (17a) is applied. The end conditions are given by

$$u|_{v=v_D} - u_D = 0 \tag{21a}$$
$$u'|_{v=v_D} - u'_D = 0 \tag{21b}$$
$$u''|_{v=v_D} - u''_D = 0 \tag{21c}$$
$$u|_{v=v_E} - u_E = 0 \tag{21d}$$

Solving the above conditions for the polynomial coefficients yields

$$g_0 = 55.4852 \quad g_1 = -0.0008 \quad g_2 = -0.1050 \quad g_3 = 0.0124 \tag{22}$$

Substituting eq. (22) into the cubic polynomial gives the desired undercutting curve. Similarly, we generate the undercutting curve around the concavity point by means of a fourth-order polynomial, as given in eq. (16a). The regions around the cusp and the concavity are shown in Fig. 10(a); a zoom-in of the two regions before and after undercutting is shown in Figs. 10(b) and (c), respectively. In these figures, the cusp point and the concavity point are indicated, correspondingly, as A and B. The undercutting curves achieve position continuity, first- and second-order geometric continuity at the blending points, and position continuity at the offset points.

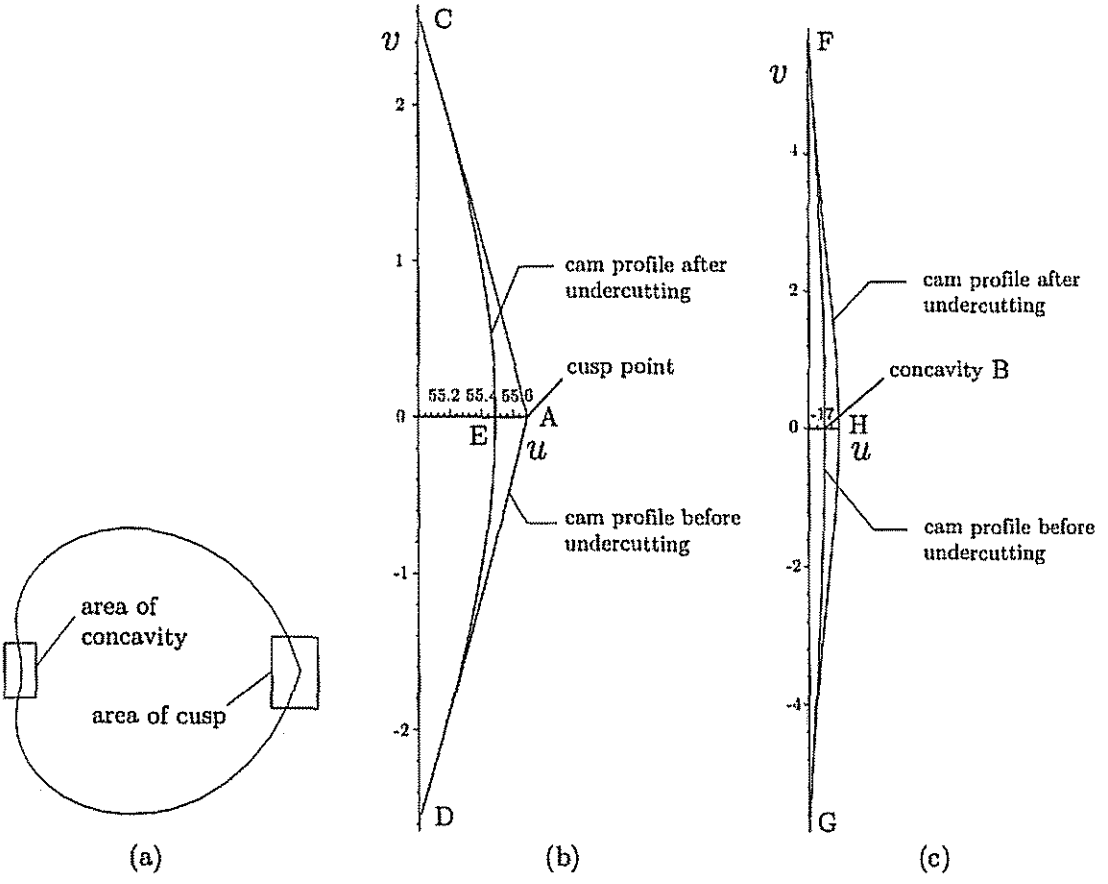

Figure 10: (a) Cam profile layout, and the curves before and after undercutting: (b) around the cusp point A and (c) around the concavity B

7 CONCLUSIONS

We analyzed the cam-based transmission, and defined the contact ratio of SoC. Undercutting on cam profiles was used to improve the transmission quality in cam-based speed-reducers. Two principles for undercutting are established to ensure a high-quality cam mechanism. One example is given to illustrate the cam profile after undercutting.

ACKNOWLEDGMENTS

The research work reported here was supported by NSERC (Science and Engineering Research Canada) under Strategic Project No. STP0192750. The FQRNT (Fonds de Recherche sur la Nature et les Technologies) Doctorate Scholarship and the ASME-Quebec Chapter Scholarship granted to the first author is given due acknowledgement.

References

[1] K. C. Gupta and J. L. Wiederrich. On the modification of cam-type profiles. *Mechanism and Machine Theory*, 21(5):439–444, 1986.

[2] R. T. Farouki, J. Manjunathaiah, and S. Jee. Design of rational cam profiles with pythagorean-hodograph curves. *Mechanism and Machine Theory*, 33(6):669–682, August 1998.

[3] S. C. Yang. Determination of spherical cam profiles by envelope theory. *Journal of Materials Processing Technology*, 116(2–3):128–136, October 2001.

[4] M.A. González-Palacios and J. Angeles. *Cam Synthesis.* Kluwer Academic Publishers, Dordrecht, Boston, London, 1993.

[5] M.A. González-Palacios and J. Angeles. The design of a novel mechanical transmission for speed reduction. *ASME J. of Mechanical Design*, 121(4):538–543, 1999.

[6] C.P. Teng. *Structure Optimization Under Variable Loading Conditions.* Doctorate Thesis, McGill University, Montreal, 2003.

[7] W. Zhang. *Cam-Profile Optimization by Means of Undercutting in Cam-Roller Speed Reducers.* Master Thesis, McGill University, Montreal, 2003.

[8] M.K. Lee. *Design for Manufacturability of Speed-Reduction Cam Mechanisms.* Master Thesis, McGill University, Montreal, 2001.

[9] S.H. Aronhold. Outline of kinematic geometry. *Verhandlungen des Vereins zur Beförderung des Gewerbefleißes in Preußen*, 51:129–155, 1872.

[10] A.B.W. Kennedy. *Mechanics of Machinery.* Macmillan, London, 1886.

[11] C.E. Wilson and J.P. Sadler. *Kinematics and Dynamics of Machinery.* Harper-Collins, 2003.

APPENDIX

The pressure angle is defined as that comprised between the direction of the unit normal to the pitch surface and the direction of the velocity of the follower at the contact point. The unit normal is written as

$$\mathbf{n} = \frac{\mathbf{u}}{\|\mathbf{u}\|}; \quad \mathbf{u} \equiv \frac{\partial \mathbf{r}_p}{\partial \psi} \times \frac{\partial \mathbf{r}_p}{\partial \lambda} \tag{23}$$

where ψ and λ are the two coordinates describing the pitch surface, with ψ defined already as the cam angular displacement, and λ measured along the generatrix of the ruled surface."

On the other hand, the unit vector w parallel to the follower velocity at points on I_{43} is obtained as

$$\mathbf{w} = \frac{\boldsymbol{\xi}}{\|\boldsymbol{\xi}\|}; \quad \boldsymbol{\xi} \equiv \boldsymbol{\omega} \times \mathbf{r}_p \tag{24}$$

where ω is the angular velocity of the follower.

Thus, the pressure angle is derived as

$$\tan \mu = \frac{\|\mathbf{n} \times \mathbf{w}\|}{\mathbf{n}^T \mathbf{w}} \tag{25}$$

The derivation of the expression for the pressure angle in spatial mechanisms is rather lengthy to be included in a research paper. Here we give a summary of the derivations in [4]. These rely on the auxiliary variables k_1, k_3, k_4, h_5 and h_6—intermediate variables are not needed in the definition of the pressure angle; those needed are left with their original indices for ease of derivation. For quick reference, these variables are reproduced below:

$$k_1 = \cos\alpha_1 \cos\alpha_3 - \sin\alpha_1 \sin\alpha_3 \cos\phi \tag{26a}$$
$$k_3 = \sin\alpha_1 \cos\alpha_3 + \cos\alpha_1 \sin\alpha_3 \cos\phi \tag{26b}$$
$$k_4 = \sin\alpha_3 \cos\alpha_1 + \cos\alpha_3 \sin\alpha_1 \cos\phi \tag{26c}$$
$$h_5 = k_1 - \phi' \cos\alpha_3 \tag{26d}$$
$$h_6 = k_4 - \phi' \sin\alpha_3 \tag{26e}$$
$$u_1 = a_1 k_1 - a_3 \cos\phi h_5 - \lambda \sin\alpha_3 \sin\phi h_5 \tag{26f}$$
$$u_2 = -a_3 \cos\alpha_1 \sin\phi h_5 + \lambda[\cos\alpha_1 \cos\phi \sin\alpha_3 h_5 + \sin\alpha_1(\phi' + \cos\alpha_3 h_5)] \tag{26g}$$
$$u_3 = \sin\phi(a_1 \sin\alpha_3 - a_3 \sin\alpha_1 h_5) + \lambda(1 - k_1 h_5 - \phi' \cos\alpha_1) \tag{26h}$$

From eq. (24), we have

$$\mathbf{w} = \frac{1}{\|\boldsymbol{\xi}\|} \begin{bmatrix} -a_3 \sin\phi + \lambda \sin\alpha_3 \cos\phi \\ a_3 \cos\alpha_1 \cos\phi + \lambda \sin\alpha_3 \cos\alpha_1 \sin\phi \\ a_3 \sin\alpha_1 \cos\phi + \lambda \sin\alpha_1 \sin\alpha_3 \sin\phi \end{bmatrix} \tag{27}$$

Moreover, the cross product appearing in eq. (25) is computed as

$$\mathbf{n} \times \mathbf{w} = \frac{\lambda^2 \mathbf{d} + \lambda \mathbf{f} + \mathbf{g}}{\|\boldsymbol{\xi}\| \|\mathbf{u}\|} \tag{28}$$

In the case of planar cam mechanisms, we have

$$\alpha_1 = \alpha_3 = 0 \tag{36a}$$
$$k_1 = 1 \tag{36b}$$
$$k_3 = 0 \tag{36c}$$
$$h_5 = 1 - \phi' \tag{36d}$$
$$h_6 = 0 \tag{36e}$$

Furthermore, all components appearing in eq. (29) become zero, except for g_3, which reduces to

$$g_3 = a_3[a_3(\phi' - 1) - a_1 \cos\phi] \tag{37}$$

Consequently, the expression for the pressure angle for planar cam mechanisms takes on the form

$$\tan\mu = \frac{a_3(\phi' - 1) - a_1 \cos\phi}{a_1 \sin\phi} \tag{38}$$

where the components of vectors $\mathbf{d}$, $\mathbf{f}$ and $\mathbf{g}$, in frame $\mathcal{F}_1$, are given below:

$$d_1 = -\sin^2\alpha_3 \sin\phi h_6 \tag{29a}$$
$$d_2 = \sin\alpha_3[\sin\alpha_1 \sin\alpha_3 h_5 + \cos\phi(\cos\alpha_1 \sin\alpha_3 h_6 + \sin^2\alpha_1)] \tag{29b}$$
$$d_3 = \sin\alpha_3[\sin\alpha_3(\cos\phi \sin\alpha_1 h_6 - \cos\alpha_1 h_5) - \cos\alpha_1 \cos\phi \sin\alpha_1] \tag{29c}$$
$$f_1 = -\sin\alpha_3(a_1 \cos\alpha_1 \sin\alpha_3 \sin^2\phi + a_3 \cos\phi h_6) \tag{29d}$$
$$f_2 = \sin\phi[a_1 \cos\alpha_1 \sin\alpha_3 k_3 - a_3(1 - \phi' \cos\alpha_1 - \cos\alpha_1 \cos\alpha_3 h_5)] \tag{29e}$$
$$f_3 = -\sin\phi[a_1 \cos\alpha_1 \sin\alpha_3 k_1 - a_3(\phi' \sin\alpha_1 + \sin\alpha_1 \cos\alpha_3 h_5)] \tag{29f}$$
$$g_1 = -a_1 a_3 \cos\alpha_1 \cos\phi \sin\alpha_3 \sin\phi \tag{29g}$$
$$g_2 = a_3[a_3 \sin\alpha_1 h_5 - a_1(\sin\alpha_3 - \cos\phi \cos\alpha_1 k_3)] \tag{29h}$$
$$g_3 = a_3 \cos\alpha_1(-a_1 \cos\phi k_1 - a_3 h_5) \tag{29i}$$

Then, $\|\mathbf{n} \times \mathbf{w}\|$ can be written as

$$\|\mathbf{n} \times \mathbf{w}\| = \frac{\sqrt{A\lambda^4 + B\lambda^3 + C\lambda^2 + D\lambda + E}}{\|\xi\|\|\mathbf{u}\|} \tag{30}$$

in which

$$A = \|\mathbf{d}\|^2 \tag{31a}$$
$$B = 2\mathbf{d}^T\mathbf{f} \tag{31b}$$
$$C = \|\mathbf{f}\|^2 + 2\mathbf{d}^T\mathbf{g} \tag{31c}$$
$$D = 2\mathbf{f}^T\mathbf{g} \tag{31d}$$
$$E = \|\mathbf{g}\|^2 \tag{31e}$$

Furthermore, the denominator of the right-hand side of eq. (25) can be expressed as

$$\mathbf{n}^T\mathbf{w} = \frac{F\lambda^2 + G\lambda + H}{\|\xi\|\|\mathbf{u}\|} \tag{32}$$

where

$$F = \sin\alpha_1 \sin\alpha_3 \sin\phi \tag{33a}$$
$$G = a_3 \cos\phi \sin\alpha_1 + a_1 \sin\alpha_3(\sin\alpha_1 \sin\alpha_3 - \cos\alpha_1 \cos\alpha_3 \cos\phi) \tag{33b}$$
$$H = a_1 a_3 \cos\alpha_1 \cos\alpha_3 \sin\phi \tag{33c}$$

Thus, the general expression for the pressure angle is given by

$$\tan\mu = \frac{\sqrt{A\lambda^4 + B\lambda^3 + C\lambda^2 + D\lambda + E}}{F\lambda^2 + G\lambda + H} \tag{34}$$

The pressure angle for spherical cams is derived from eq. (34) by taking $\lambda \to \infty$, i.e.,

$$\tan\mu = \lim_{\lambda\to\infty} \frac{\sqrt{A\lambda^4 + B\lambda^3 + C\lambda^2 + D\lambda + E}}{F\lambda^2 + G\lambda + H} = \frac{(\phi' - \cos\alpha_1)\sin\alpha_3 - \sin\alpha_1 \cos\alpha_3 \cos\phi}{\sin\alpha_1 \sin\phi} \tag{35}$$